Atmospheric Environment 43 (2009) 4453–4464

Contents lists available at ScienceDirect

Atmospheric Environment

journal homepage: www.elsevier.com/locate/atmosenv

Using atmospheric chemistry and storm track information to explain the variation of nitrate stable isotopes in precipitation at a site in central Pennsylvania, USA

Anthony R. Buda [a,b,*], David R. DeWalle [c]

[a] USDA Agricultural Research Service, Building 3702, Curtin Road, University Park, PA 16802, USA
[b] Penn State University, 132 Land and Water Research Building, University Park, PA 16802, USA
[c] Penn State University, 311 Forest Resources Building, University Park, PA 16802, USA

ARTICLE INFO

Article history:
Received 16 December 2008
Received in revised form
12 June 2009
Accepted 15 June 2009

Keywords:
Nitrate sources
Stable isotope tracers
Precipitation chemistry
Storm tracks
Atmospheric oxidants

ABSTRACT

Stable isotopes of NO_3^- ($\delta^{15}N$–NO_3^- and $\delta^{18}O$–NO_3^-) were monitored in precipitation at a central Pennsylvania site during six storm events in 2005 to determine whether information on atmospheric oxidants (e.g., O_3, NO_2, and NO_x), and storm tracks (using the NOAA HYSPLIT model) were capable of explaining observed seasonal and within-storm isotopic variation. Results showed that $\delta^{15}N$–NO_3^- and $\delta^{18}O$–NO_3^- in precipitation varied significantly during individual storm events. Seasonally, $\delta^{15}N$–NO_3^- and $\delta^{18}O$–NO_3^- in precipitation followed a pattern of depletion during the summer months and enrichment during the winter months. NO_3^- precursor concentrations and atmospheric oxidants were useful for explaining the seasonal and within-storm variation of $\delta^{15}N$–NO_3^- for all six storm events as evidenced by negative relationships with NO_2:NO_x ratios and ozone (O_3). In comparison, $\delta^{18}O$–NO_3^- was positively related to O_3 in three dormant season storms, which suggested that the O_3 oxidation pathway was important for producing the high $\delta^{18}O$–NO_3^- observed in wintertime precipitation. Storm track information was especially useful for describing differences in $\delta^{15}N$–NO_3^-. Cool-sector storms originating from the E/NE produced slightly negative $\delta^{15}N$–NO_3^- values characteristic of automobile emissions, whereas warm-sector storms with tracks from the SW/S/SE produced slightly positive $\delta^{15}N$–NO_3^- values characteristic of coal-fired emissions. Lightning also may have been an important source of atmospheric NO_3^- during two warm-sector thunderstorms. This study showed that (1) information about oxidant levels can be useful to predict the seasonal and within-storm variation of NO_3^- stable isotopes in precipitation, and (2) knowledge of storm tracks (warm-sector versus cool-sector) may be important for determining sources of NO_3^- in wet deposition.

© 2009 Elsevier Ltd. All rights reserved.

1. Introduction

Stable isotopes of nitrogen (^{15}N) and oxygen (^{18}O) are increasingly being used to understand the sources and cycling of nitrate (NO_3^-) in precipitation and its fate as wet deposition in terrestrial and aquatic ecosystems (Kendall et al., 2007). Much of this interest is driven by the fact that NO_3^- is major component of acidic deposition, which has altered nutrient cycles in eastern U.S. forests (Likens et al., 1996) and impaired water quality in acid-sensitive headwater streams (Kahl et al., 2004). Additional motivation for isotope studies of NO_3^- in precipitation has been generated because wet deposited nitrogen (N), of which NO_3^- is a significant component, may account for as much as 30% of the total N load delivered to estuarine systems such as the Chesapeake Bay (Castro et al., 2003).

The majority of the research on ^{15}N and ^{18}O isotopes in precipitation NO_3^- (referred to as $\delta^{15}N$–NO_3^- and $\delta^{18}O$–NO_3^- from this point forward) has focused on two major themes: (1) assessing the significance of atmospheric processes and pollutant sources that may affect $\delta^{15}N$–NO_3^- and $\delta^{18}O$–NO_3^- values (Hastings et al., 2003; Elliott et al., 2007), and (2) using $\delta^{18}O$–NO_3^- as a tracer to quantify the contribution of atmospheric wet NO_3^- deposition in nitrogen-limited forest ecosystems (Williard et al., 2001) and to evaluate the importance of atmospheric NO_3^- sources during high stream flow periods in mixed land-use (Chang et al., 2002) and urbanized watersheds (Ging et al., 1996). It is in the context of each of these types of studies that temporal variation (e.g., within-storm, seasonal, etc.) of $\delta^{15}N$–NO_3^- and $\delta^{18}O$–NO_3^- in precipitation must be considered.

* Corresponding author at: USDA Agricultural Research Service, Building 3702, Curtin Road, University Park, PA 16802, USA. Tel.: +1 814 865 6623; fax: +1 814 863 0935.
E-mail address: anthony.buda@ars.usda.gov (A.R. Buda).

1352-2310/$ – see front matter © 2009 Elsevier Ltd. All rights reserved.
doi:10.1016/j.atmosenv.2009.06.027

Of the types of variation anticipated for $\delta^{15}N–NO_3^-$ and $\delta^{18}O–NO_3^-$ stable isotopes in precipitation, seasonal variation has received by far the most attention in the literature. Many studies have documented seasonal variation in $\delta^{15}N–NO_3^-$ and $\delta^{18}O–NO_3^-$ (see Kendall et al., 2007 and references therein) in atmospheric and precipitation NO_3^- at various sites around the world. In general, $\delta^{15}N–NO_3^-$ and $\delta^{18}O–NO_3^-$ values are highest during the winter months and lowest during the summer months. An exception for $\delta^{15}N–NO_3^-$ was found at a site in Bermuda, where the highest $\delta^{15}N–NO_3^-$ values occurred during the warm season (April–September) and the lowest $\delta^{15}N–NO_3^-$ values occurred during the cool season (October–March) (Hastings et al., 2003). Recent explanations for seasonal variation in $\delta^{15}N–NO_3^-$ and $\delta^{18}O–NO_3^-$ have centered on seasonal shifts in prevailing oxidant chemistry in the atmosphere (e.g., OH versus O_3 concentrations) and the associated effects on different NO_3^- precursor concentrations (e.g., NO, NO_2 and NO_x) (Hastings et al., 2003).

In contrast to seasonal variation of $\delta^{15}N–NO_3^-$ and $\delta^{18}O–NO_3^-$, much less is known about how these isotopes vary during storm events. Early work by Moore (1973), Heaton and Collett (1985), and Heaton (1987) identified within-storm variation of $\delta^{15}N–NO_3^-$. Based on limited samples, the authors generally concluded that the within-storm variation was not consistent on a storm-to-storm basis. Heaton (1987) suggested that variations of $\delta^{15}N–NO_3^-$ during storms in Pretoria, South Africa may have been due to selective washout of N bearing compounds. Other mechanisms may also have been important, but these have yet to be thoroughly explored. With regard to $\delta^{18}O–NO_3^-$, no published studies were found that have documented within-storm variation. Some evidence for the possibility of $\delta^{18}O–NO_3^-$ variation during storms stems from the results of a study conducted in central Pennsylvania, where ^{18}O in water ($\delta^{18}O–H_2O$ from this point forward) was shown to vary greatly during the course of 10 different storm events sampled in 1989 and 1990 (Pionke and DeWalle, 1992). $\delta^{18}O–H_2O$ is potentially related to $\delta^{18}O–NO_3^-$ because $\delta^{18}O–H_2O$ has been shown to influence the ^{18}O of hydroxyl radicals (OH) in the atmosphere (Dubey et al., 1997). OH is an important oxidant involved in atmospheric NO_3^- formation (Calvert et al., 1985) and contributes oxygen (O) atoms to newly formed NO_3^- molecules. As a result of this known relationship, we anticipate that $\delta^{18}O–NO_3^-$ also would vary during storm events, although the exact mechanisms responsible (e.g., importance of OH versus O_3) for the variation would require further exploration.

While seasonal variation and within-storm variation are clearly important for $\delta^{15}N–NO_3^-$ and $\delta^{18}O–NO_3^-$, storm origin and atmospheric conditions also may result in observable effects on these isotopes as suggested by several recent studies (Russell et al., 1998; Cooney, 2005). For example, Russell et al. (1998) collected bulk precipitation samples from 60 storm events at a site near Lewes, DE at the mouth of the Delaware Bay from 1993 through 1994 and analyzed them for $\delta^{15}N–NO_3^-$. Back trajectory analysis using the NOAA HYbrid Single-Particle Lagrangian Integrated Trajectory (HYSPLIT) model (see Draxler and Hess, 2004) showed that transport patterns originating from the northwest and west of Lewes, DE produced the highest fluxes of NO_3^- and had $\delta^{15}N–NO_3^-$ values indicative of fossil fuel combustion. Hastings et al. (2003) collected precipitation samples on an event basis on the island of Bermuda from 2000 through 2001 and analyzed the samples for $\delta^{15}N–NO_3^-$ and $\delta^{18}O–NO_3^-$. Results using back trajectory analysis showed that air masses with origins from the southeast and southwest produced higher $\delta^{15}N–NO_3^-$ and lower $\delta^{18}O–NO_3^-$ isotope ratios than air masses originating from the north and northwest. Further, the two general groups of transport patterns to Bermuda were well correlated with air mass conditions, with warm season (April–September) air masses exhibiting southeast and southwest transport patterns and cool season (October–March) air masses exhibiting north and northwest transport patterns. More recently, Cooney (2005) analyzed $\delta^{15}N–NO_3^-$ and $\delta^{18}O–NO_3^-$ in precipitation for 46 storm event samples of bulk precipitation collected from 2002 through 2004 at a site in Frederick, MD. Unlike the previous studies, no relationship between storm origin and NO_3^- stable isotopes could be identified using back trajectory analysis. Clearly, other factors may be important in addition to storm origin to explain the variability of $\delta^{15}N–NO_3^-$ and $\delta^{18}O–NO_3^-$ in precipitation samples.

Additional insight may be gained from studies combining back trajectory analysis and atmospheric air mass characterization to help explain the variation of stable isotopes in water for different types of storm tracks. Studies in central New York State conducted by Lawrence et al. (1982) using deuterium (δD) and Burnett et al. (2004) using $\delta^{18}O–H_2O$ showed that these isotope ratios generally were lowest in the cool-sector of storms and highest in the warm-sector of storms. The positioning of frontal boundaries and low pressure systems relative to the sites in central New York primarily determined the temperature of the air mass and the resultant isotope ratios for δD and $\delta^{18}O–H_2O$. It appears that characterizing storm track patterns and air mass conditions together may help further explain storm-to-storm variation in $\delta^{15}N–NO_3^-$ and $\delta^{18}O–NO_3^-$ in precipitation.

The overall goal of this study was to characterize the stable nitrate isotope ($\delta^{15}N–NO_3^-$ and $\delta^{18}O–NO_3^-$) and inorganic chemical composition of precipitation for six different storm events at a site located within the Spring Creek watershed in central Pennsylvania. Specific study objectives were to (1) assess the significance of inter- and intra-storm variation of NO_3^- stable isotopes, (2) utilize available information on atmospheric oxidant (e.g., O_3) and NO_3^- precursor concentrations (e.g., NO_x and NO_2) to help explain the variation of NO_3^- stable isotopes in precipitation, and (3) use surface weather maps and back trajectory analysis to test the hypothesis that storm origin and atmospheric air mass conditions result in observable differences in the NO_3^- stable isotopic composition of precipitation.

2. Materials and methods

2.1. Study site location and description

Precipitation samples were collected at a single station located within the Spring Creek watershed in central Pennsylvania (Fig. 1). Spring Creek is a 371 km^2 mixed land-use watershed, which is situated within the Nittany Valley in the Valley and Ridge physiographic region. Central Pennsylvania has a humid, temperate climate, with average annual precipitation approximately 97 cm based upon 80 years of data (1926–2005) measured at State College, PA (Pennsylvania State Climatologist, 2006). During the period of study (2005), the total observed precipitation for the year was 1040 mm, which was 7% above the long-term mean. The precipitation sampling site was established adjacent to the Land and Water Research Building in University Park, PA (40.81°N, −77.85°W). All precipitation samples were collected on a storm event basis.

2.2. Precipitation collection

Six storm events (Table 1) were sampled using a passive precipitation sampler designed and constructed to collect sufficient volumes of rainwater for NO_3^- stable isotope and inorganic chemical analysis. The sampler was constructed from a polyethylene plastic tarp, approximately 5.7 m^2 in area, which funneled water to a series of three 20-L polypropylene carboys (Fig. 2). A new tarp was used for each event that was sampled, and the tarp was washed three times with deionized water just prior to the onset of precipitation. Carboys were arranged such that they filled sequentially during storms according to a slightly modified design from that of Kennedy et al. (1979). Approximately 3.6 mm (0.14 in) of rainfall filled an individual

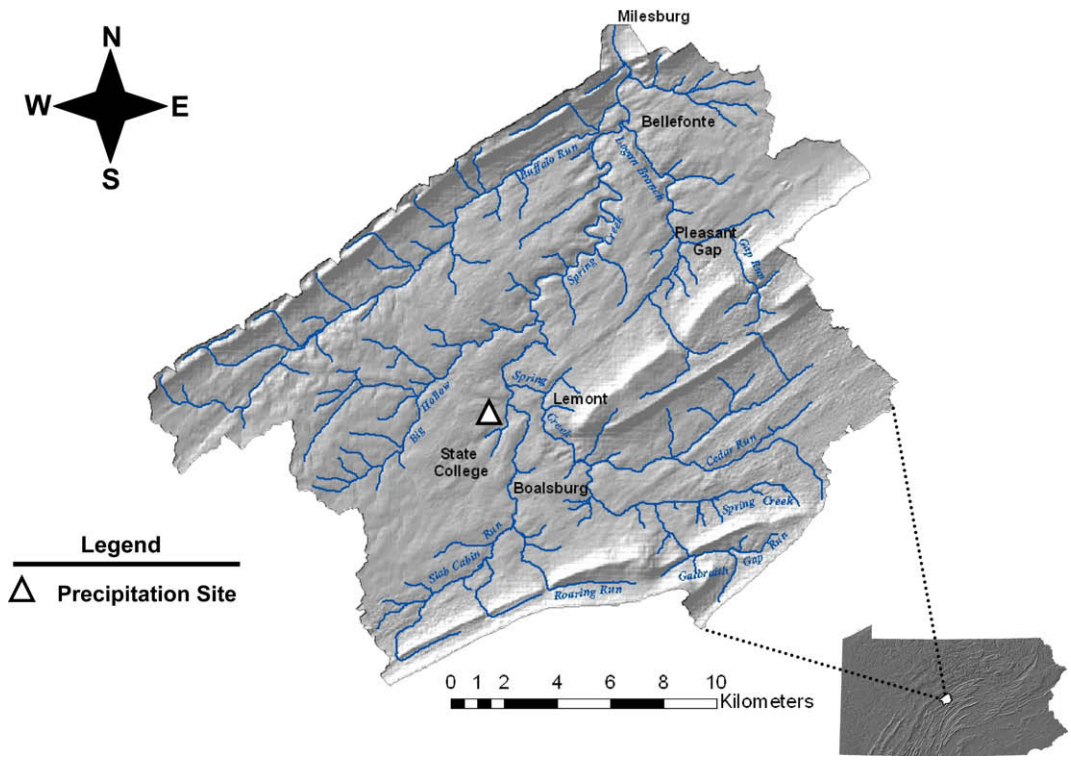

Fig. 1. Map showing general location where precipitation samples were collected within the Spring Creek watershed.

carboy. Once three sequential carboys were filled with rainwater (~10.8 mm of rainfall), three clean carboys were brought in to replace the full ones. This process was repeated so that the within-storm variation of stable isotopes and chemistry could be evaluated. During large rain events (>29 mm), precipitation samples typically had to be integrated to some degree because these events produced more rainwater than what could be sampled using 8 carboys. Furthermore, high-intensity rainfall during two thunderstorms resulted in some short-circuiting of the funnel and tube connections.

2.3. Water chemistry and stable isotope analyses

Precipitation samples were analyzed for inorganic chemistry at the Water Quality Laboratory in the Penn State Institutes of Energy and the Environment (PSIEE). All water samples were filtered through 0.45 μm filters. Water samples were analyzed for pH, specific conductance, and nitrate–N (NO_3–N). All analyses were conducted using standard methods (APHA, 2005).

Stable isotopes in NO_3^- ($\delta^{15}N$–NO_3^- and $\delta^{18}O$–NO_3^-) were analyzed according to the methods outlined by Chang et al. (1999) and Silva et al. (2000). Briefly, anion exchange resins were used to collect dissolved NO_3^- in all water samples. Spoelstra et al. (2004) showed that samples of precipitation NO_3^- could be stored for up to two weeks with minimal effects of biological isotope fractionation. During the course of the study, all precipitation samples were filtered onto anion exchange resins within one week of collection. Anion exchange resins loaded with NO_3^- were stored at 4 °C until they could be shipped to the University of Waterloo Environmental Isotope Laboratory (EIL) for further processing and analysis. More specific details on the analytical methods used by the University of Waterloo EIL are given in Spoelstra et al. (2004). The results for $\delta^{15}N$–NO_3^- and $\delta^{18}O$–NO_3^- are reported in delta notation ($\delta^{15}N$ and $\delta^{18}O$ in permil units, ‰) versus their respective international reference standards: N_2 gas for $\delta^{15}N$–NO_3^- and Standard Mean Ocean Water (SMOW) for $\delta^{18}O$–NO_3^-. The analytical error for both isotopes was approximately ±0.2‰ based on duplicate samples (26 duplicates for $\delta^{15}N$–NO_3^- and 14 duplicates for $\delta^{18}O$–NO_3^-).

$\delta^{18}O$–H_2O also was analyzed at the University of Waterloo EIL. Water samples for $\delta^{18}O$–H_2O were collected and stored in airtight 20-mL HDPE scintillation bottles prior to shipment to the EIL at

Table 1
Relevant characteristics of the six storms sampled during 2005 in central PA.

Storm	Date	Description	Duration (hrs)	Precipitation characteristics				Storm classifications	
				Type	Amount (mm)	Mean intensity (mm hr^{-1})	Number of samples	Predominant storm track	Air mass type
1	03-23-05	Low pressure and frontal passage	10	Rain/Snow	12.2	1.0	3	E/NE	Cool-sector
2	03-28-05	Coastal storm/Nor'easter	32	Rain	61.0	2.0	8	E/NE	Cool-sector
3	07-05-05	Thunderstorm	2	Rain	35.4	18.0	2	S/SW	Warm-sector
4[a]	08-31-05	Thunderstorm	1	Rain	49.0	49.0	2	SE	Warm-sector
5[b]	10-07-05	Low pressure and frontal passage	13	Rain	87.0	6.7	5	SE	Warm-sector
6	11-16-05	Cold frontal passage	5	Rain	13.7	2.7	3	S	Warm-sector

[a] Remnants of hurricane Katrina.
[b] Remnants of tropical storm Tammy.

Fig. 2. Precipitation sampler used to collect sequential precipitation samples for water chemistry and stable isotope analyses.

Waterloo. The analysis for $\delta^{18}O–H_2O$ was conducted using the CO_2 equilibration method outlined by Epstein and Mayeda (1953). All results are reported in delta notation ($\delta^{18}O$ in permil units, ‰) relative to Standard Mean Ocean Water (SMOW). The analytical error for $\delta^{18}O–H_2O$ isotopes was approximately ±0.1‰ based on 20 duplicate samples.

2.4. Storm characterization and back trajectories

All sampled storms were characterized using available meteorological data to assess the potential influence of air mass and storm tracks on NO_3^- stable isotopes and precipitation chemistry. Weather surface maps for the continental U.S. were obtained from the National Weather Service (NWS) Hydrometeorological Prediction Center (HPC) map archive (NWS, 2006) for each of the six storm events sampled during 2005. These maps were used to characterize the general synoptic conditions for each event. The location of the cold frontal boundary was used to define whether State College remained in the cold-sector or the warm-sector of the storm (Lawrence et al., 1982). If the storm track occurred along a cold front that had not yet passed through State College, the storm was classified as a warm-sector storm. On the other hand, if a storm moved along a cold frontal boundary that had already passed through State College, then the storm was classified as a cool-sector storm.

In addition to using surface weather maps, back trajectories were computed with Version 4 of the HYSPLIT model (see Draxler and Hess, 2004; NOAA, 2006) using data from the Eta Data Assimilation System (EDAS – 40 km resolution). Back trajectories were calculated at 500 m above ground level (agl), which is within the atmospheric boundary layer. Back trajectories were traced for 48 h just prior to the end of each storm.

2.5. Climate and atmospheric chemistry data

Climate and atmospheric chemistry data were collected for the duration of each storm event to help explain the variation in measurements of stable isotopes and inorganic chemicals in precipitation. Total precipitation amounts were monitored using a simple rain gauge attached to the precipitation sampler. Hourly precipitation and temperature data were obtained from a NWS weather station located at the nearby University Park (UP) Airport (NCDC, 2006). Hourly nitrogen oxide (NO_2 and NO_x) data were obtained from the Air Quality Learning and Demonstration Center located on the Penn State University campus (PA DEP, 2006), and hourly O_3 data were obtained from the Clean Air Status and Trends Network (CASTNET) Leading Ridge monitoring site (EPA, 2006) located about 17 km south of State College. All hourly data were aggregated to obtain a representative observation of climate and atmospheric chemistry conditions for each precipitation chemistry sample taken during a storm event (Table 2).

3. Results and discussion

3.1. Storm descriptions and characterization

A total of six storms were sampled during the 2005 calendar year (see Table 1 for details). The storms were characterized according to storm track (see Fig. 3a–f) and classified as cool-sector or warm-sector storms (Table 1). A more complete description of each storm event is given in Buda (2007).

3.2. Inter-storm and seasonal variation

3.2.1. $\delta^{15}N–NO_3^-$

The mean $\delta^{15}N–NO_3^-$ value for each event varied throughout the 2005 study period (Table 2, Fig. 4a). According to Fig. 4a, $\delta^{15}N–NO_3^-$ began to decline from the March 23 storm (mean = −0.1‰) to its lowest value, which was recorded during the July 5 storm (mean = −2.9‰). $\delta^{15}N–NO_3^-$ was much higher on August 31 (mean = +0.6‰) and then reached its peak on October 7 (mean = +2.5‰). It remained elevated on the November 16 storm (mean = +1.6‰). A distinct seasonal pattern in $\delta^{15}N–NO_3^-$ is apparent in the precipitation dataset.

Seasonal patterns of $\delta^{15}N–NO_3^-$ have been demonstrated by many investigators (see Kendall et al., 2007 and references therein). Essentially, $\delta^{15}N–NO_3^-$ in precipitation is lowest during the summer and peaks sometime during the autumn and winter months. In general, the same pattern of variation for $\delta^{15}N–NO_3^-$ in precipitation was observed in central Pennsylvania using data from the six storm events sampled in 2005. Further, the range of variability in this study using mean values (−2.9‰ in mid summer to +2.5‰ in early fall) compared favorably to the range of variability observed by Cooney (2005) in Maryland (−3‰ in summer to +2.5‰ in fall). One notable exception to the seasonal pattern of $\delta^{15}N–NO_3^-$ was observed in Bermuda precipitation, where Hastings et al. (2004) reported the highest $\delta^{15}N–NO_3^-$ in the spring and the lowest $\delta^{15}N–NO_3^-$ in the late autumn during the course of a one-year study. While several investigators have used oxidant chemistry and variations in NO_2 and NO_x to explain seasonal differences in the $\delta^{15}N–NO_3^-$ in precipitation (Freyer et al., 1993), Hastings et al. (2004) postulated that changes in air mass and pollutant sources were more likely responsible for the seasonal differences in $\delta^{15}N–NO_3^-$ in precipitation on Bermuda.

3.2.2. $\delta^{18}O–NO_3^-$

Mean $\delta^{18}O–NO_3^-$ values for each storm exhibited seasonal variation that generally was similar to the pattern of variation observed for $\delta^{15}N–NO_3^-$ (Table 2, Fig. 4b). $\delta^{18}O–NO_3^-$ increased from the storm on March 23 (mean = +37.6‰) to the storm on March 28–29 (mean = +51.6‰), and then decreased substantially to its lowest value during the thunderstorms on July 5 (mean = +19.7‰). After July 5, $\delta^{18}O–NO_3^-$ in precipitation steadily increased through the storms on August 31 (mean = +26.9‰) and October 7 (mean = +40.6‰), reaching its peak value on November 16 (mean = +51.9‰). A similar seasonal trend to $\delta^{15}N–NO_3^-$ was noted. Organizing the storm data according to dormant season (March 23, March 28–29, November 16) and growing season (July 5, August 31, October 7) events also showed differences in $\delta^{18}O–NO_3^-$, with dormant season $\delta^{18}O–NO_3^-$ (+48.7‰)

Table 2
Climate, precipitation chemistry, stable isotopic composition, and atmospheric chemistry for all samples collected during the 2005 precipitation study. The row in italics represents the results from a melted snow sample on 3-23-05.

Storm	Date	Climate		Precipitation chemistry			Stable isotopes			Atmospheric chemistry		
		Precip (mm)	Air temp (°C)	pH	Cond.[a] (μS cm^{-1})	NO_3^- (mg L^{-1})	$\delta^{18}O$–NO_3^- (‰)	$\delta^{15}N$–NO_3^- (‰)	$\delta^{18}O$–H_2O (‰)	O_3 (ppb)	NO_2 (ppb)	NO_x (ppb)
Storm 1	3/23	4.6	2.3	4.5	18.8	3.3	+40.6	+0.4	−11.0	27.7	10.0	10.7
	3/23	5.1	1.0	4.3	30.4	2.2	NES[b]	NES[b]	−11.9	34.8	9.0	10.0
	3/23	2.5	1.0	*5.2*	*3.8*	*0.4*	*+34.7*	*−0.6*	*−16.7*	*31.0*	*10.0*	*11.0*
Storm 2	3/28	6.1	6.1	4.2	34.5	2.2	+70.0	−2.5	−8.6	46.3	7.5	7.8
	3/28	14.7	5.0	4.5	15.2	0.5	+50.5	−1.8	−8.3	42.0	5.0	5.0
	3/28	1.8	4.3	4.7	10.7	0.6	+44.5	−5.1	−9.5	42.0	4.0	4.0
	3/28	0.3	3.0	4.7	11.7	0.7	+53.0	−3.5	−7.9	39.3	6.8	7.0
	3/28	12.2	3.2	4.8	9.0	0.3	+42.8	+1.8	−8.1	25.0		
	3/28	6.6	4.9	4.7	11.7	0.5	+34.9	+1.8	−9.2	24.3		
	3/28	11.2	6.0	4.6	13.8	0.5	+49.2	+3.2	−10.4	32.3		
	3/28	8.1	6.1	4.9	7.3	0.8	+67.7	−5.6	−11.2	36.6		
Storm 3	7/5	19.1	19.5	4.5	21.0	1.4	+19.7	−2.9	−4.9	45.7	3.0	3.7
	7/5	16.3	19.0	4.5	17.2	0.6			−5.7	39.0	3.0	4.0
Storm 4	8/31	5.8	23.0	4.2	17.5	1.0	+11.9	+5.0	−3.6	24.0	5.0	6.0
	8/31	43.2	22.0	4.7	8.6	0.4	+41.9	−3.8	−4.7	31.0	4.0	4.5
Storm 5	10/7	9.1	18.5	5.2	4.0	0.2	+46.0	+2.3	−5.1	15.0	9.0	12.0
	10/7	13.2	19.0	5.3	2.5	0.3	+35.6	+3.0	−5.8	21.3	11.3	17.3
	10/7	34.8	19.0	5.5	1.9	0.2	+30.7	+4.0	−8.2	21.3	8.7	10.7
	10/7	27.9	19.0	5.3	2.7	0.3	+44.6	+0.4	−9.2	18.7	8.3	10.0
	10/7	2.0	19.0	5.4	2.8	0.3	+46.2	+2.8	−8.9	20.0	9.5	11.0
Storm 6	11/16	6.9	18.0	5.6	7.5	0.8	+60.9	+2.4	−5.5	31.5	3.5	4.5
	11/16	2.0	16.5	6.1	2.8	0.3	+40.1	+0.6	−8.5	29.5	4.0	5.0
	11/16	4.8	13.5	6.7	15.9	0.7	+54.8	+1.9	−7.3	29.5	4.5	6.0

Italics = results obtained from a melted snow sample.
[a] Cond. = Electrical conductivity.
[b] NES = Not enough sample.

being significantly higher than growing season $\delta^{18}O$–NO_3^- (+39.3‰) ($p = 0.013$) based on a two-tailed *t*-test.

The seasonality of $\delta^{18}O$–NO_3^- in precipitation has been widely reported by many researchers in different locations around the world (see Kendall et al., 2007 and references therein). For $\delta^{18}O$–NO_3^-, the lowest values typically occur during the summer months and the highest values occur during the winter months. This basic pattern of variability also was observed during 2005 in central Pennsylvania using data from six storm events. The magnitude of variation for $\delta^{18}O$–NO_3^- in precipitation in central Pennsylvania was +19.7‰ to +51.91‰ using mean values for each storm, which encompasses a small portion of the total range of values for $\delta^{18}O$–NO_3^- in precipitation reported by Kendall (1998) for sites in North America and Germany (+14‰ to +71‰). If the full range of values from this study are considered (+11.9‰ to +69‰), then a larger portion of the range reported by Kendall (1998) is accounted for. While the value of +11.9‰ for $\delta^{18}O$–NO_3^- may indeed represent one of the lower values among previously reported observations for sites in North America, it also may be possible that this value is merely a reflection of the sealed glass tube method (see Révész and Böhlke, 2002) used to analyze $\delta^{18}O$–NO_3^- in this study (see Kendall et al., 2007 for a more thorough discussion of this issue).

3.3. Intra-storm variation

3.3.1. $\delta^{15}N$–NO_3^-

$\delta^{15}N$–NO_3^- exhibited substantial variation during the course of individual storm events (Table 2). The magnitude of the intra-storm variations in $\delta^{15}N$–NO_3^- ranged from about 1‰ to greater than 8‰ for all six storms (mean = 4.8‰). The maximum change in $\delta^{15}N$–NO_3^- was 8.8‰ and it occurred during the March 28–29 storm event.

Few studies have documented the types of changes in $\delta^{15}N$–NO_3^- that might occur during storms. Moore (1973) showed isotopic changes of about 1‰ for $\delta^{15}N$–NO_3^- sampled from a storm event near Boulder, CO. He tentatively noted that the $\delta^{15}N$–NO_3^- increased as concentrations of NO_3^- increased during the storm. Later, Heaton and Collett (1985) and Heaton (1987) sampled a series of storms near Pretoria, South Africa and documented fairly large changes in $\delta^{15}N$–NO_3^- (~2–9‰) during different events. Unlike Moore (1973), Heaton (1987) did not observe any distinct relationships between $\delta^{15}N$–NO_3^- and NO_3^- concentrations during events. Relationships between $\delta^{15}N$–NO_3^- and NO_3^- concentrations were observed during the course of individual storm events in the current study, although these relationships were quite weak.

Patterns of $\delta^{15}N$–NO_3^- variation during storms also were assessed for each event. For the two storms sampled during 2005 with 5 or more precipitation samples, the patterns of $\delta^{15}N$–NO_3^- variation were very different (Figs. 5a and 6a). For the storm on March 28–29, $\delta^{15}N$–NO_3^- increased slightly at the beginning of the storm (+0.7‰), dropped during the mid-point of the event (−3.3‰), and then increased considerably (+8.3‰) before dropping substantially again (−8.8‰) toward the end of the storm. On October 7, $\delta^{15}N$–NO_3^- increased gradually throughout the event (+1.7‰), fell moderately (−3.5‰) and then increased again (+2.2‰) at the end of the storm. These results are in contrast to Heaton (1987), who, with the exception of one event, reported that $\delta^{15}N$–NO_3^- generally followed an increasing pattern during storms. Both Moore (1973) and Heaton (1987) suggested that atmospheric oxidation reactions may have caused the observed $\delta^{15}N$–NO_3^- variations in precipitation, but did not have the data available to test those hypotheses. The potential effects of climate and atmospheric chemistry on $\delta^{15}N$–NO_3^- variations are explored later in this paper.

3.3.2. $\delta^{18}O$–NO_3^-

During the study, substantial variation in $\delta^{18}O$–NO_3^- ranging from +6.7 to +35.1‰ was observed during individual storm

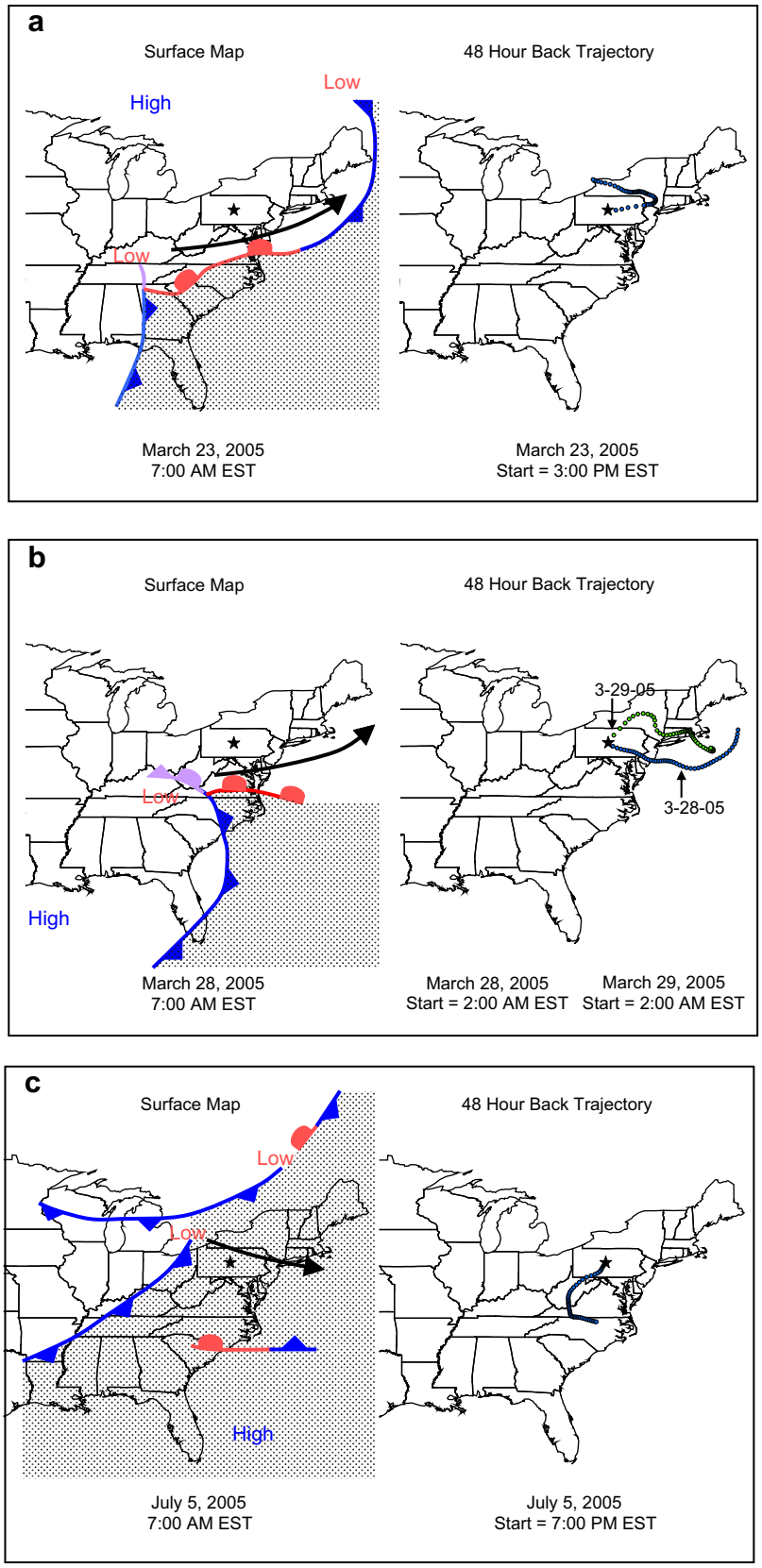

Fig. 3. (a–f): Weather surface maps (left) and 48-h back trajectories (right) at 500 m above ground level for storms sampled on (a) March 23, 2005; (b) March 28–29, 2005; (c) July 5, 2005; (d) August 31, 2005; (e) October 7, 2005; (f) November 16, 2005. On both panels, the star indicates the location of the collection site in State College, PA. On the left-hand panel, the heavy black arrow indicates forward movement of storm system and the shaded region indicates the location of the warm-sector of the storm. On the right-hand panel, start times for the 48-h back trajectory are given for each storm.

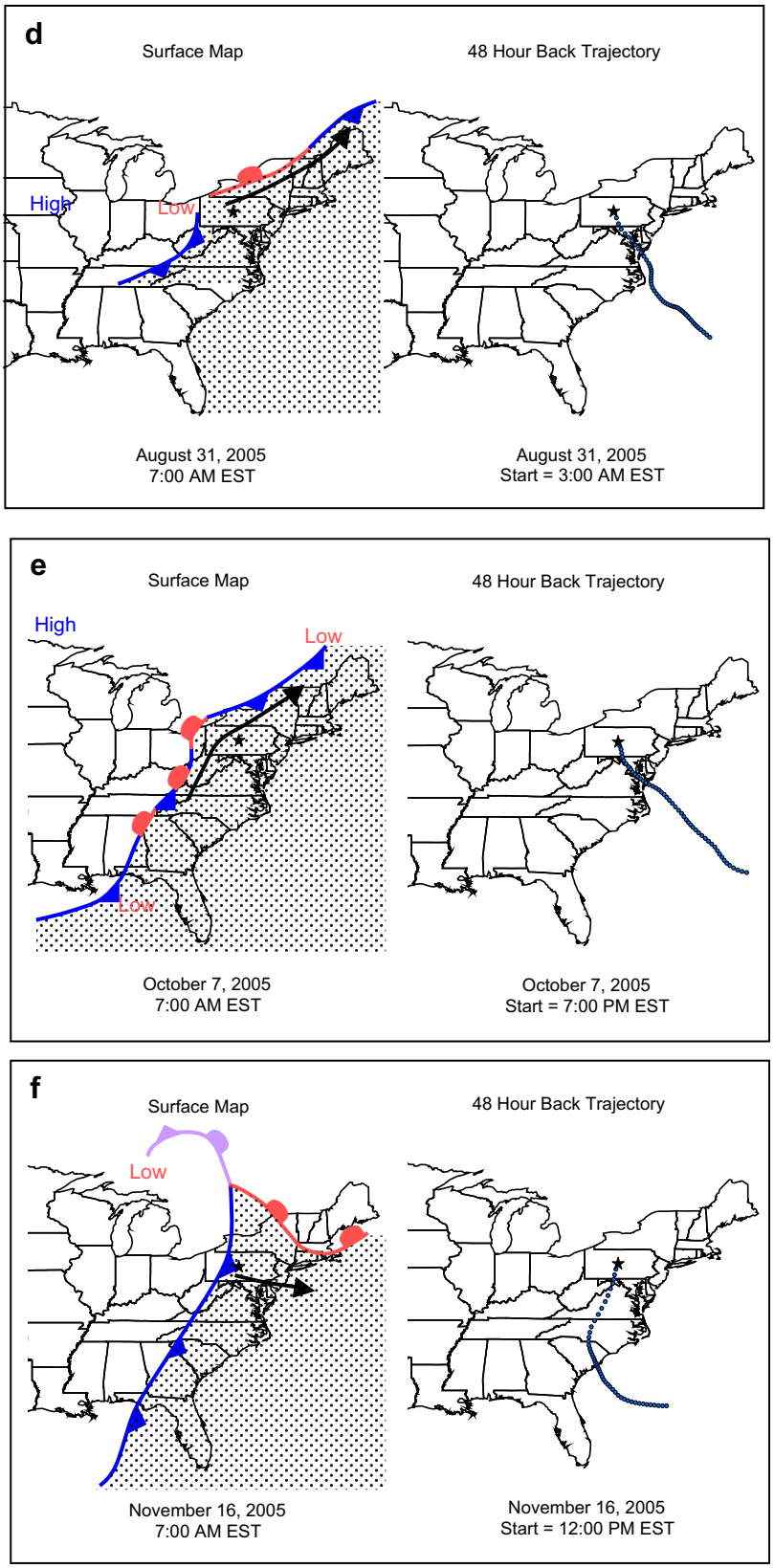

Fig. 3. (*Continued*)

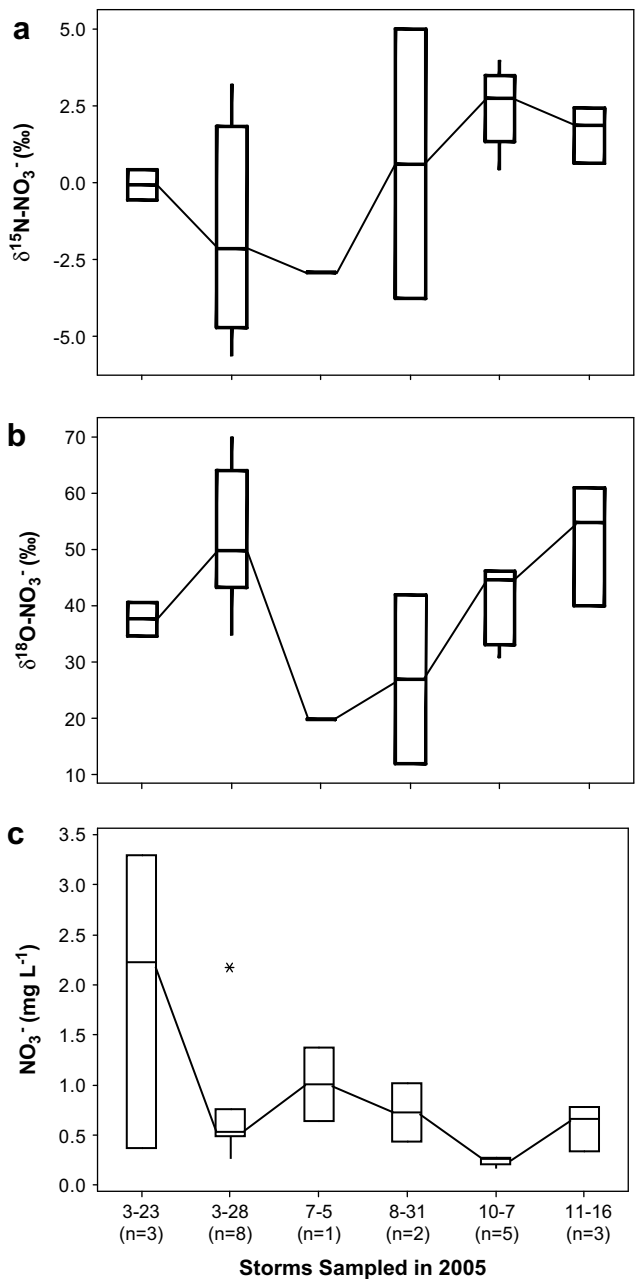

Fig. 4. Box plots of (a) $\delta^{15}N–NO_3^-$ (‰), (b) $\delta^{18}O–NO_3^-$ (‰), and (c) NO_3^- (mg L^{-1}) in precipitation for all six storms sampled during 2005.

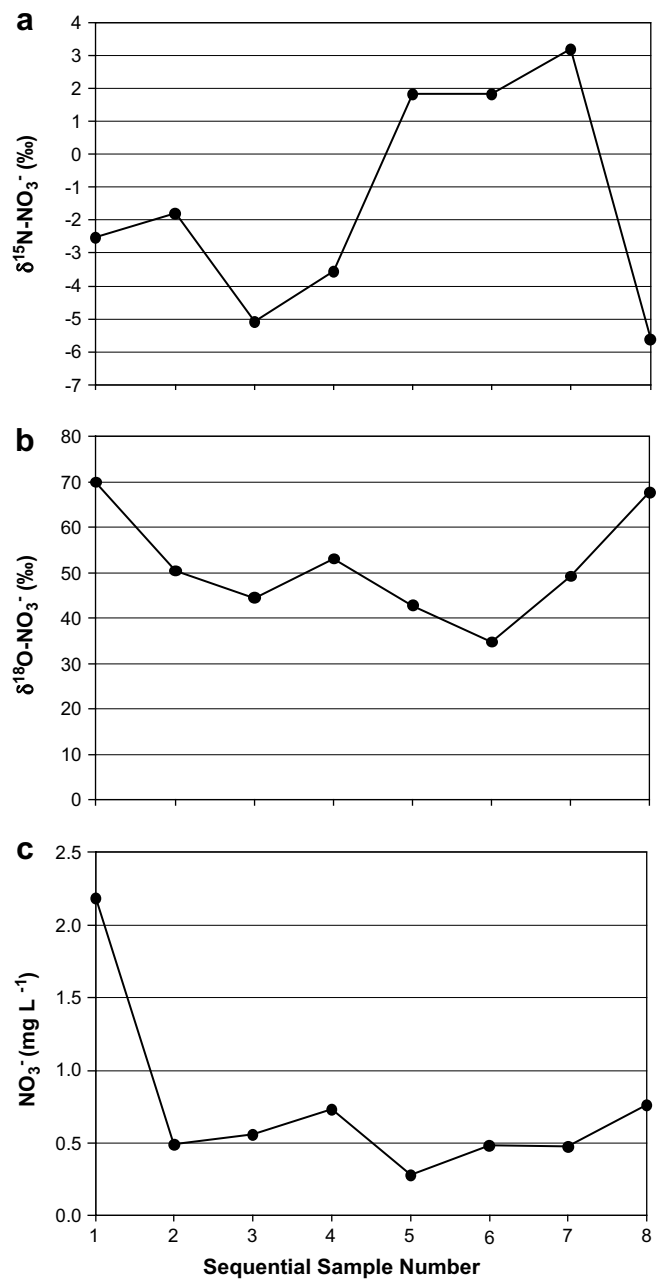

Fig. 5. Within-storm variation in (a) $\delta^{15}N–NO_3^-$ (‰), (b) $\delta^{18}O–NO_3^-$ (‰), and (c) NO_3^- (mg L^{-1}) in precipitation for the storm event sampled on March 28–29, 2005.

events (mean = +21.5‰) (Table 2). The maximum change in $\delta^{18}O–NO_3^-$ occurred during the March 28–29 storm event, which was the longest duration event sampled during 2005. Interestingly, the magnitude change in $\delta^{18}O–NO_3^-$ was not related to the size or duration of the storm event, with the second largest change (30.0‰) occurring during the shortest duration event (August 31).

Patterns of $\delta^{18}O–NO_3^-$ changes during storms appeared to be more systematic than patterns of $\delta^{15}N–NO_3^-$ (Table 2). For the three storms that were sampled where greater than 3 samples were collected for $\delta^{18}O–NO_3^-$ (March 28–29, October 7, and November 16), $\delta^{18}O–NO_3^-$ typically was enriched at the beginning of the event, decreased as the storm progressed, and then increased to a value similar to the starting isotopic composition. $\delta^{18}O–NO_3^-$ trends are shown for the storms sampled on March 28–29 (Fig. 5b) and October 7 (Fig. 6b). A plot of NO_3^- concentration variation is also showed for the same two storm events (Figs. 5c and 6c). From the two plots, it appears that $\delta^{18}O–NO_3^-$ and NO_3^- concentrations vary together during storms. Pearson correlation analysis showed that correlation coefficients between $\delta^{18}O–NO_3^-$ and NO_3^- concentrations were 0.55 ($p < 0.001$) and 0.39 ($p < 0.001$) for the March 28–29 and October 7 storms, respectively. The reason for these correlations is not known, but like $\delta^{15}N–NO_3^-$, the atmospheric processes responsible for NO_3^- formation may be an important driver.

To our knowledge, no published studies have documented the variation of $\delta^{18}O–NO_3^-$ during individual storms. The variation of $\delta^{18}O–NO_3^-$ is primarily significant in the context of tracing atmospheric NO_3^- in wet deposition. Measurements of $\delta^{18}O–NO_3^-$ in bulk

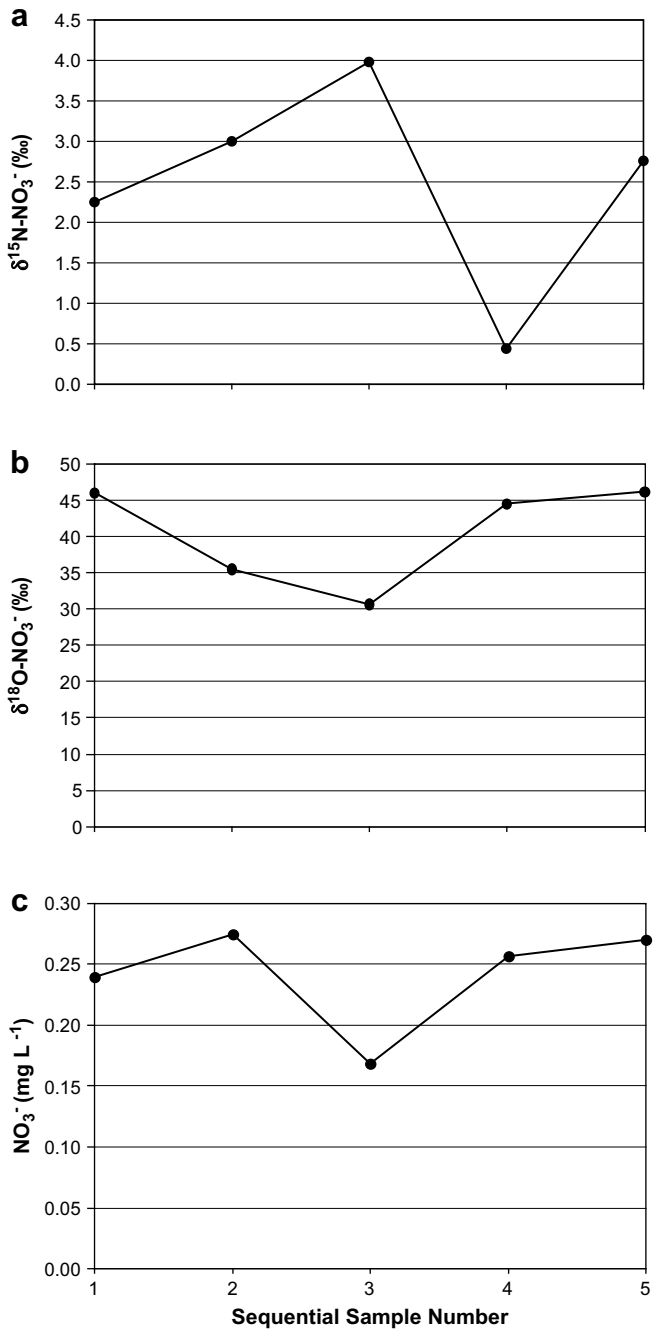

Fig. 6. Within-storm variation in (a) $\delta^{15}N–NO_3^-$ (‰), (b) $\delta^{18}O–NO_3^-$ (‰), and (c) NO_3^- (mg L^{-1}) in precipitation for the storm event sampled on October 7, 2005.

precipitation are used in two-component mixing models to estimate the percent contribution of wet NO_3^- deposition to total stream water NO_3^- in forested watersheds (e.g., Williard et al., 2001). In general, studies of this nature have concluded that wet NO_3^- deposition accounts for anywhere from 30 to 50% of the total NO_3^- in stream water in forested watersheds, with NO_3^- from soil nitrification making up the remaining 50–70%. Since the degree to which $\delta^{18}O–NO_3^-$ varies in rainfall is not usually known for a given event, the range of possible solutions using two-component mixing models is rarely if ever reported. Therefore, care should be taken when interpreting the reported contributions of wet NO_3^- deposition to total stream water NO_3^- in light of the variation of precipitation $\delta^{18}O–NO_3^-$ reported herein.

3.4. Possible explanations for observed $\delta^{15}N–NO_3^-$ variation

Several possible controls on the variation of $\delta^{15}N–NO_3^-$ were explicitly considered in the context of this study, including (1) effects of atmospheric oxidation chemistry on the formation of NO_3^-, (2) possible changes in the sources of atmospheric NO_3^-, and (3) storm track and air mass characteristics. The potential importance of lightning also was explored, as lightning can be an important source of NO_3^- in precipitation (Hastings et al., 2003).

Some evidence has been presented to suggest that atmospheric oxidation chemistry may explain the seasonal variation of $\delta^{15}N$ in NO_2 gas (Freyer et al., 1993), and thus potentially the $\delta^{15}N$ of the resultant HNO_3 (Hastings et al., 2004). In a study performed in Jülich, Germany, Freyer et al. (1993) showed that the cyclic reactions responsible for converting between NO and NO_2 affected the $\delta^{15}N$ value of NO_2 gas. The seasonality of $\delta^{15}N$ in NO_2 was attributed to changes in the ratio of NO_2 to NO_x (NO_2:NO_x), where NO_x is defined as the sum of NO and NO_2. Freyer et al. (1993) argued that the large equilibrium isotope effect between NO and NO_2 ($\alpha = 1.028$ at 25 °C) becomes more pronounced as the ratio of NO_2:NO_x approaches 1 during the winter months. This in turn would be expected to produce higher values of $\delta^{15}N$ in NO_2. During the summer months, when more complete oxidation of NO to NO_2 occurs due to higher concentrations of O_3, the ratio of NO_2:NO_x increases, decreasing the influence of the isotopic exchange reaction between NO_2 and NO_x and producing lower values of $\delta^{15}N$ in NO_2 (Freyer et al., 1993).

Hourly data on atmospheric concentrations of NO_2 and NO_x were available from the Air Quality Learning and Demonstration Center at Penn State, and were used to determine whether the ratio of NO_2:NO_x could explain the observed inter- and intra-storm variations of $\delta^{15}N–NO_3^-$ in precipitation in central Pennsylvania. Fig. 7a shows a significant ($p = 0.002$, $R^2 = 0.47$) negative relationship between $\delta^{15}N–NO_3^-$ and NO_2:NO_x. The slope of this relationship (−21) compared favorably to the slopes reported by Freyer et al. (1993) (−16 to −22) for the reported relationships between $\delta^{15}N$ in NO_2 and NO_2:NO_x. Further support for the effects of oxidation reactions on $\delta^{15}N–NO_3^-$ can be seen in Fig. 7b, which shows a significant ($p < 0.001$, $R^2 = 0.54$) negative relationship between $\delta^{15}N–NO_3^-$ and atmospheric O_3. Freyer et al. (1993) observed that $\delta^{15}N–NO_3^-$ in precipitation was often highest when O_3 concentrations were lowest during the winter months, and the relationship in Fig. 7b is consistent with this observation. The relationships in Fig. 7a and b suggest that changes in the atmospheric oxidation chemistry, including effects on the ratio of NO_2 to NO_x and atmospheric concentrations of O_3, help explain observed changes in the $\delta^{15}N–NO_3^-$ in precipitation both during and in between storm events in central Pennsylvania.

Changes in anthropogenic and natural sources of atmospheric NO_3^- also have been suggested as possible drivers for the variation of $\delta^{15}N–NO_3^-$ in precipitation (e.g., Elliott et al., 2007). Heaton (1990) reported that the $\delta^{15}N$ of NO_x resulting from vehicle exhaust emissions ranged from −13‰ to −2‰, whereas the $\delta^{15}N$ of NO_x from coal combustion ranged from +6‰ to +9‰. In addition, the $\delta^{15}N$ of NO_x derived from the use of animal manures in large-scale agricultural operations is likely to be very negative (<<0‰) due to the preferential volatilization of ^{14}N isotopes. In terms of natural NO_x, soil emissions, biomass burning, and lightning all represent important potential sources, with lightning being particularly important during the summer months in the northeast U.S. (Price et al., 1997). While little is known about the $\delta^{15}N$ of NO_x emitted from soils and biomass burning (Kendall et al., 2007), a study of natural NO_x produced by simulated lightning (Hoering, 1957) suggested that $\delta^{15}N$ values could range between −0.5‰ and +1.4‰. For this particular study, it is possible that mixtures of NO_3^- from vehicle emissions, coal-fired power plant emissions, and agricultural land-use emissions affected $\delta^{15}N–NO_3^-$ in rainfall during all six storms in

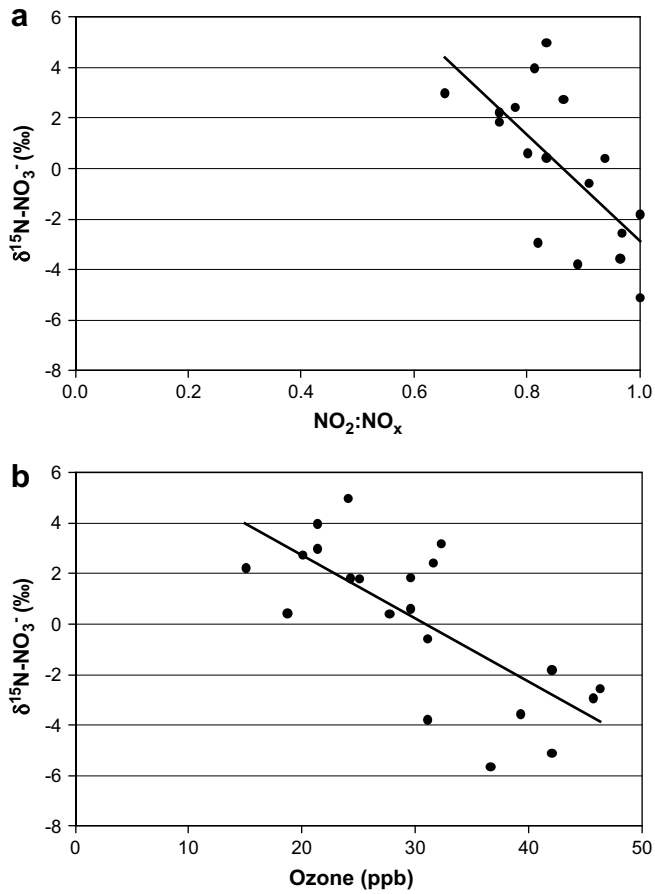

Fig. 7. Plots of δ^{15}N–NO_3^- (‰) in precipitation versus (a) NO_2:NO_x and (b) ozone (ppb) for all six storms sampled during 2005. The regression equation for δ^{15}N–NO_3^- (‰) versus NO_2:NO_x is: $Y = -21X + 18$ ($p = 0.002$, $R^2 = 0.47$). The regression equation for δ^{15}N–NO_3^- (‰) versus ozone (ppb) is: $Y = -0.3X + 7.8$ ($p < 0.001$, $R^2 = 0.54$).

central Pennsylvania, with lightning representing a potentially important fourth source during the two thunderstorms on July 5 and August 31. The relative importance of these sources is explored further in the context of storm origin and air mass characteristics.

Back trajectory analysis and air mass characterization were used to assess whether there were any effects of air mass source on δ^{15}N–NO_3^- that might indicate a change in the source of NO_3^- in precipitation. In essence, the two storms in March were characterized by east/northeast (E/NE) transport patterns with precipitation occurring in the cool-sector of the storm (Fig. 3a and b). In contrast, the four storms that followed were characterized by southwest/south/southeast SW/S/SE transport patterns and produced precipitation in the warm-sector of the storm (Fig. 3c–f). Table 3 shows that δ^{15}N–NO_3^- was significantly lower ($p = 0.051$) for storms with E/NE transport and cool-sector precipitation (−1.2‰) as compared to storms with SW/S/SE transport and warm-sector precipitation (+1.4‰). Thus, storms occurring with transport patterns from the E/NE exhibited negative δ^{15}N–NO_3^- values that may have been influenced by NO_x derived from automobile emissions or other natural sources with negative δ^{15}N–NO_3^- values. Storms with SW/S/SE transport patterns over the Ohio River Valley exhibited positive δ^{15}N–NO_3^- values that were greater than those measured in storms with E/NE transport patterns. While this indicated a stronger influence of NO_3^- from coal-fired power plant emissions and/or lightning (July 5 and August 31 thunderstorms), influences from agricultural emissions also cannot be ruled out since two storms in particular (July 5 and November 16) had 48-h back trajectories that

Table 3
Comparison of precipitation amount, inorganic chemistry, and stable isotope characteristics of cool-sector and warm-sector storm events.

	Cool sector E/NE transport ($n = 11$)[a]	Warm sector SW/S/SE transport ($n = 12$)
Mean rainfall (mm)	29.8	36.3
Mean NO_3^- concentration (mg L^{-1})	1.06	0.53
Mean NO_3^- deposition (kg ha^{-1})	0.06	0.08
δ^{15}N–NO_3^- (‰)[b]	−1.19	1.42
δ^{18}O–NO_3^- (‰)	48.79	39.30

[a] n = number of samples collected during cool-sector and warm-sector storms.
[b] Results of a one-way ANOVA were significant at $\alpha = 0.10$.

tracked through the intensive agricultural regions of the southeast U.S. Ultimately, these conclusions should be interpreted with care, as they are based upon the limited available information on δ^{15}N values in atmospheric NO_3^- sources reported in the literature.

3.5. Possible explanations for observed δ^{18}O–NO_3^- variation

The variation of δ^{18}O–NO_3^- in precipitation, especially due to changes in season, primarily has been explained in the context of different atmospheric oxidation pathways. Simplified atmospheric reactions responsible for producing HNO_3 from NO_x in the atmosphere are summarized below (Calvert et al., 1985; Hastings et al., 2004).

Summertime Reactions

$$NO_2 + h\nu \longrightarrow NO + O$$
$$NO + O_3 \longrightarrow NO_2 + O_2$$
$$NO_2 + OH + M \longrightarrow HNO_3 + M$$

Wintertime Reactions

$$NO_2 + O_3 \longrightarrow NO_3 + O_2$$
$$NO_2 + NO_3 + M \longrightarrow N_2O_5 + M$$
$$N_2O_5 + H_2O \xrightarrow{\text{aerosol}} 2HNO_3$$

Reactions during the summertime are dominated by the oxidation of NO_x via OH. During the wintertime, when OH concentrations are typically lower than in summer, the oxidation of NO_x is dominated by O_3. The δ^{18}O value of OH is expected to reflect the isotopic composition of H_2O vapor (Dubey et al., 1997), which is typically negative. O_3 on the other hand has δ^{18}O values in the range of +90‰ to +122‰ (Johnston and Thiemens, 1997). As a result, oxidation of NO_2 via the OH pathway influences the lower δ^{18}O–NO_3^- observed during the summer months. In contrast, reactions between NO_x and O_3 during the wintertime influence the higher values of δ^{18}O–NO_3^-. This process helps to explain the seasonal (storm-to-storm) variation of δ^{18}O–NO_3^- observed in precipitation during 2005 in central Pennsylvania (Fig. 4b).

Further evidence was sought to verify the importance of these different reaction pathways by using available information on atmospheric O_3 concentrations and the δ^{18}O–H_2O value of rainwater. δ^{18}O–NO_3^- data for all six storms were classified according to the time of year that the precipitation occurred. Wintertime (dormant season) storms included the events on March 23, March 28–29, and November 16. Summertime (growing season) storms included the events on July 5, August 31, and October 7. A significant ($p = 0.02$, $R^2 = 0.49$) and positive relationship was found between δ^{18}O–NO_3^- and O_3 concentrations (ppb) for the three storms that occurred during the winter months, when oxidation via the O_3 pathway would be expected to dominate (Fig. 8a). Thus, as O_3 becomes progressively more available to oxidize NO_x to HNO_3 in the troposphere, δ^{18}O–NO_3^- in precipitation increases. In contrast, during the summertime, a non-significant negative relationship ($p = 0.15$, $R^2 = 0.31$) was found between δ^{18}O–NO_3^- and δ^{18}O–H_2O in precipitation (Fig. 8b). While the relationship was not statistically significant at the $\alpha = 0.05$ level, it does suggest that δ^{18}O–H_2O may

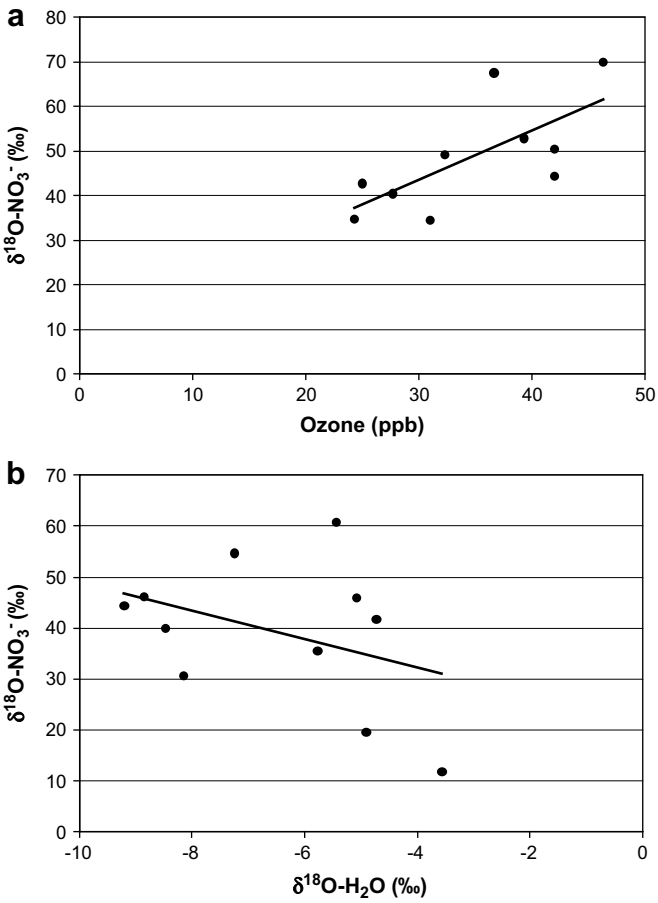

Fig. 8. Plots of $\delta^{18}O–NO_3^-$ (‰) in precipitation versus (a) ozone (ppb) for storms occurring during the dormant season ($n = 3$ storms) and (b) $\delta^{18}O–H_2O$ (‰) in precipitation for storms occurring during the growing season ($n = 3$ storms). The regression equation for $\delta^{18}O–NO_3^-$ (‰) versus ozone (ppb) is: $Y = 1.1X + 10.5$ ($p = 0.024$, $R^2 = 0.49$). The regression equation for $\delta^{18}O–NO_3^-$ (‰) versus $\delta^{18}O–H_2O$ (‰) is: $Y = -2.8X + 21$ ($p = 0.15$, $R^2 = 0.31$).

be useful for inferring the effects of OH oxidation on $\delta^{18}O–NO_3^-$. Certainly, this hypothesis would require further exploration.

The influence of storm track and air mass characteristics also were investigated as possible controls on the $\delta^{18}O–NO_3^-$ in precipitation. While $\delta^{18}O–NO_3^-$ in precipitation was higher for storms that exhibited east/northeast (E/NE) transport patterns (cool-sector) than for storms that exhibited southwest/south/southeast (SW/S/SE) transport patterns (warm-sector), the difference was not statistically significant ($p = 0.12$). Thus, unlike $\delta^{15}N–NO_3^-$, storm track and air mass characteristics did not help to explain observed differences in $\delta^{18}O–NO_3^-$.

4. Conclusions

Significant inter- and intra-storm variation of $\delta^{15}N–NO_3^-$ and $\delta^{18}O–NO_3^-$ in precipitation was observed during six storms sampled during 2005 in central Pennsylvania. $\delta^{15}N–NO_3^-$ and $\delta^{18}O–NO_3^-$ were most depleted during the summer months and were most enriched during winter. Patterns of $\delta^{15}N–NO_3^-$ variation during two long-duration storms were very different. In contrast, $\delta^{18}O–NO_3^-$ variation followed a pattern of enrichment at the beginning and ending of storms, with the most depleted values occurring during the middle of the event. $\delta^{15}N–NO_3^-$ decreased with increasing ratios of NO_2:NO_x and O_3 in the atmosphere, which suggested that atmospheric oxidation chemistry was an important driver of seasonal and within-storm variation of these isotopes. $\delta^{18}O–NO_3^-$ variations during three dormant season storm events were positively related to O_3, which implied that the O_3 oxidation pathway was important for producing the high $\delta^{18}O–NO_3^-$ observed in wintertime precipitation. Cool-sector storms with tracks from the E/NE produced slightly negative $\delta^{15}N–NO_3^-$ values characteristic of automobile emissions, whereas warm-sector storms with tracks from the SW/S/SE produced slightly positive $\delta^{15}N–NO_3^-$ values characteristic of coal-fired emissions. No relationship between $\delta^{18}O–NO_3^-$ and storm track was observed in the data. The results of this study demonstrated that: (1) information about oxidant levels can help to predict the seasonal and within-storm variation of NO_3^- stable isotopes, and (2) knowledge of storm tracks (warm-sector versus cool-sector) may be useful for determining sources of NO_3^- in wet deposition.

Acknowledgments

We wish to thank the United States Geological Survey (USGS) Pennsylvania Water Resources Research Center Grant Program (Grant 2005PA40B), the School of Forest Resources, and the Penn State Institutes of Energy and the Environment (PSIEE) for providing necessary funds to support this research. We also thank Bryan Swistock, Chad Voorhees, Shawn Rummel, Nesha Mizel, Leonard McNeal, Jennifer Sidleck, Stephanie Clemens, Scott Atkinson, and Susan Buda for help with precipitation sampling during the course of this project.

References

American Public Health Association (APHA), 2005. Standard Methods for the Examination of Water and Wastewater, 21st ed. American Public Health Association (APHA), 1368 pp.

Buda, A.R., 2007. Tracing Stream Nitrate in a Central Pennsylvania Mixed Land-use Basin Using Stable Isotopes, Bacteria, and Inorganic Chemicals. Ph.D. dissertation in Forest Resources. The Pennsylvania State University, 242 pp.

Burnett, A.W., Mullins, H.T., Patterson, W.P., 2004. Relationship between atmospheric circulation and winter precipitation $\delta^{18}O$ in central New York State. Geophysical Research Letters 31. doi:10.1029/2004GL021089.

Calvert, J.G., Lazrus, A., Kok, G.L., Heikes, B.G., Walega, J.G., Lind, J., Cantrell, C.A., 1985. Chemical mechanisms of acid generation in the troposphere. Nature 317, 27–35. doi:10.1038/317027a0.

Castro, M.S., Driscoll, C.T., Jordan, T.E., Reay, W.G., Boynton, W.R., 2003. Sources of nitrogen to estuaries in the United States. Estuaries 26 (3), 803–814. doi:10.1007/BF02711991.

Chang, C.C.Y., Langston, J., Riggs, M., Campbell, D.H., Silva, S.R., Kendall, C., 1999. A method for nitrate collection for $\delta^{15}N$ and $\delta^{18}O$ analysis from waters with low nitrate concentrations. Canadian Journal of Fisheries and Aquatic Sciences 56 (10), 1856–1864. doi:10.1139/cjfas-56-10-1856.

Chang, C.C.Y., Kendall, C., Silva, S.R., Battaglin, W.A., Campbell, D.H., 2002. Nitrate stable isotopes: tools for determining nitrate sources among different land uses in the Mississippi River Basin. Canadian Journal of Fisheries and Aquatic Sciences 59, 1874–1885. doi:10.1139/F02-153.

Cooney, K.S., 2005. A Stable Isotopic Investigation of Precipitation Nitrate. Master's of Science thesis in Geology. University of Maryland, 173 pp.

Draxler, R.D., Hess, G.D., 2004. Description of the HYSPLIT_4 modeling system. NOAA Technical Memorandum ERL ARL-224, 25 pp.

Dubey, M.K., Mohrschladt, R., Donahue, N.M., Anderson, J.G., 1997. Isotope specific kinetics of hydroxyl radical (OH) with water (H_2O): testing models of reactivity and atmospheric fractionation. Journal of Physical Chemistry 101, 1494–1500. doi:10.1021/jp962332p.

Elliott, E.M., Kendall, C., Wankel, S.D., Burns, D.A., Boyer, E.W., Harlin, K., Bain, D.J., Butler, T.J., 2007. Nitrogen isotopes as indicators of NO_x source contributions to atmospheric nitrate deposition across the Midwestern and Northeastern United States. Environmental Science and Technology 41, 7661–7667. doi:10.1021/es070898t.

Environmental Protection Agency (EPA), 2006. Clean Air Status and Trends Network (CASTNET). http://www.epa.gov/castnet/.

Epstein, S., Mayeda, T., 1953. Variation of ^{18}O content of water from natural sources. Geochimica et Cosmochimica Acta 4, 213–224.

Freyer, H.D., Kley, D., Volz-Thomas, A., Kobel, K., 1993. On the interaction of isotopic exchange processes with photochemical reactions in atmospheric oxides of nitrogen. Journal of Geophysical Research 98 (D8), 14791–14796.

Ging, P.B., Lee, R.W., Silva, S.R., 1996. Water Chemistry of Shoal Creek and Waller Creek, Austin, Texas, and Potential Sources of Nitrate. U.S. Geological Survey Water-resources Investigation Paper 96–4167.

Hastings, M.G., Sigman, D.M., Lipschultz, F., 2003. Isotopic evidence for source changes of nitrate in rain at Bermuda. Journal of Geophysical Research 108 (D24). doi:10.1029/2003JD003789.

Hastings, M.G., Steig, E.J., Sigman, D.M., 2004. Seasonal variations in N and O isotopes of nitrate in snow at Summit, Greenland: implications for the study of nitrate in snow and ice cores. Journal of Geophysical Research 109. doi:10.1029/2004JD004991.

Heaton, T.H.E., Collett, G.M., 1985. The Analysis of $^{15}N/^{14}N$ Ratios in Natural Samples, with Emphasis on Nitrate and Ammonium in Precipitation. CSIR Research Report 624. National Physical Research Laboratory. Council for Scientific and Industrial Research, Pretoria, South Africa.

Heaton, T.H.E., 1987. $^{15}N/^{14}N$ ratios of nitrate and ammonium in rain at Pretoria, South Africa. Atmospheric Environment 21 (4), 843–852. doi:10.1016/0004-6981(87)90080-1.

Heaton, T.H.E., 1990. $^{15}N/^{14}N$ ratios of NO_x from vehicle engines and coal-fired power stations. Tellus 42B, 304–307. doi:10.1034/j.1600-0889.1990.t01-1-00009.x.

Hoering, T., 1957. The isotopic composition of the ammonia and the nitrate ion in rain. Geochimica et Cosmochimica Acta 12, 97–102.

Johnston, J.C., Thiemens, M.H., 1997. The isotopic composition of tropospheric ozone in three environments. Journal of Geophysical Research 102 (C12), 26861–26875. doi:10.1029/97JD02075.

Kahl, J.S., Stoddard, J.L., Haeuber, R., Paulsen, S.G., Birnbaum, R., Deviney, F.A., Webb, J.R., DeWalle, D.R., Sharpe, W.E., Driscoll, C.T., Herlihy, A.T., Kellog, J.H., Murdoch, P.S., Roy, K., Webster, K.E., Urquhart, N.S., 2004. Have U.S. surface waters responded to the 1990 Clean Air Act Amendments? Environmental Science and Technology 38 (24), 484A–490A.

Kendall, C., 1998. Tracing nitrogen sources and cycling in catchments. In: Kendall, C., McDonnell, J.J. (Eds.), Isotope Tracers in Catchment Hydrology. Elsevier, Amsterdam, pp. 521–576.

Kendall, C., Elliott, E.M., Wankel, S.D., 2007. Tracing anthropogenic inputs of nitrogen to ecosystems. In: Lajtha, K., Michener, R.H. (Eds.), Stable Isotopes in Ecology and Environmental Science, second ed. Blackwell Scientific Publications, Oxford, pp. 375–449.

Kennedy, V.C., Zellweger, G.W., Avanzino, R.L., 1979. Variation of rain chemistry during storms at two sites in northern California. Water Resources Research 15, 687–702. doi:10.1029/WR015i003p00687.

Lawrence, J.R., Gedzelman, S.D., White, J.C., Smiley, D., Lazov, P., 1982. Storm trajectories in eastern U.S. D/H isotopic composition of precipitation. Nature 296, 638–640. doi:10.1038/296638a0.

Likens, G.E., Driscoll, C.T., Buso, D.C., 1996. Long-term effects of acid rain: response and recovery of a forest ecosystem. Science 272, 244–246. doi:10.1126/science.272.5259.244.

Moore, H., 1973. Isotopic measurement of atmospheric nitrogen compounds. Tellus 26 (1–2), 169–174.

National Climatic Data Center (NCDC), 2006. http://www.ncdc.noaa.gov/oa/ncdc.html.

National Oceanic and Atmospheric Administration (NOAA), 2006. NOAA Air Resources Laboratory (ARL) HYSPLIT Model Webpage. http://www.arl.noaa.gov/ready/hysplit4.html.

National Weather Service (NWS), 2006. NWS Hydrometeorological Prediction Center (HPC) Surface Weather Map Archive. http://www.hpc.ncep.noaa.gov/dailywxmap/frame.html.

Pennsylvania Department of Environmental Protection (PA DEP), 2006. Air Quality Learning and Demonstration Center. Penn State University. Data access: http://www.aireffects.psu.edu/learning/index.htm.

Pennsylvania State Climatologist, 2006. Pennsylvania State Climatologist, 503 Walker Building, University Park, PA 16802. http://climate.psu.edu.

Pionke, H.B., DeWalle, D.R., 1992. Intra- and inter-storm ^{18}O trends for selected rainstorms in Pennsylvania. Journal of Hydrology 138, 131–143. doi:10.1016/0022-1694(92)90160-W.

Price, C., Penner, J., Prather, M., 1997. NO_x from lightning 1. Global distribution based on lightning physics. Journal of Geophysical Research 102 (D5), 5929–5941. doi:10.1029/96JD03504.

Révész, K., Böhlke, J.K., 2002. Comparison of $\delta^{18}O$ measurements in nitrate by different combustion techniques. Analytical Chemistry 74 (20), 5410–5413. doi:10.1021/ac025854b.

Russell, K.M., Galloway, J.N., Macko, S.A., Moody, J.L., Scudlark, J.R., 1998. Sources of nitrogen in wet deposition to the Chesapeake Bay region. Atmospheric Environment 32 (14/15), 2453–2465. doi:10.1016/S1352-2310(98)00044-2.

Silva, S.R., Kendall, C., Wilkinson, D.H., Ziegler, A.C., Chang, C.C.Y., Avanzino, R.J., 2000. A new method for collection of nitrate from fresh water and the analysis of nitrogen and oxygen isotope ratios. Journal of Hydrology 228, 22–36. doi:10.1016/S0022-1694(99)00205-X.

Spoelstra, J., Schiff, S.L., Jeffries, D.S., Semkin, R.G., 2004. Effect of storage on the isotopic composition of nitrate in bulk precipitation. Environmental Science and Technology 38, 4723–4727. doi:10.1021/es030584f.

Williard, K.W.J., DeWalle, D.R., Edwards, P.J., Sharpe, W.E., 2001. ^{18}O isotopic separation of stream nitrate sources in mid-Appalachian forested watersheds. Journal of Hydrology 252, 174–188. doi:10.1016/S0022-1694(01)00459-0.